Bull. Mater. Sci., Vol. 19, No. 6, December 1996, pp. 939–956. © Printed in India.

Synthesis of nanocrystalline alloys and intermetallics by mechanical alloying

S K PABI* and B S MURTY
Department of Metallurgical and Materials Engineering, Indian Institute of Technology, Kharagpur 721 302, India

Abstract. Nanocrystalline Al_3Ni, NiAl and Ni_3Al phases in Ni–Al system and the α, β, γ, ε and deformation induced martensite in Cu–Zn system have been synthesized by mechanical alloying (MA) of elemental blends in a planetary mill. Al_3Ni and NiAl were always ordered, while Ni_3Al was disordered in the milled condition. MA results in large extension of the NiAl and Ni_3Al phase fields, particularly towards Al-rich compositions. Al_3Ni, a line compound under equilibrium conditions, could be synthesized at nonstoichiometric compositions as well by MA. The phases obtained after prolonged milling (30 h) appear to be insensitive to the starting material for any given composition > 25 at.% Ni. The crystallite size was finest (~ 6 nm) when NiAl and Ni_3Al phases coexisted after prolonged milling. In contrast, in all Cu–Zn blends containing 15 to 85 at.% Zn, the Zn-rich phases were first to form, and the final crystallite sizes were coarser (15–80 nm). Two different modes of alloying have been identified. In case of NiAl and Al_3Ni, where the ball milled product is ordered, as well as, the heat of formation (ΔH_f) is large (> 120 kJ/mol), a rapid discontinuous mode of alloying accompanied with an additive increase in crystallite size is detected. In all other cases, irrespective of the magnitude of ΔH_f, a gradual diffusive mode of intermixing during milling seems to be the underlying mechanism of alloying.

Keywords. Mechanical alloying; nanocrystals; synthesis; Al–Ni; Cu–Zn.

1. Introduction

The nanostructured solids exhibit noble properties like high strength and toughness, exceptionally high diffusivity and sinterability, unusual formability in conventionally brittle materials at ambient temperatures (Gleiter 1992; Koch 1993; Das and Pabi 1996). These enhanced properties are generally attributed to their large grain boundary volume (Gleiter 1992). However, recent high resolution electron microscopic results (Neiman *et al* 1991) have suggested that the volume of the 'grain boundary phase' may not be appreciable in these materials.

Mechanical alloying (MA) is a high energy ball milling technique, pioneered by Benjamin (1970) in the early seventies. It has now established itself as a viable solid state processing route for the synthesis of novel materials (Koch 1991; Murty 1993). MA is an economic route of producing large quantities of nanostructured materials with good control over multicomponent product composition and homogeneity.

Intermetallic compounds, such as, aluminides have attracted the attention of many investigators (Miracle 1993; Noebe *et al* 1993) due to their high specific strength and high temperature capabilities. The possibility of improving the room temperature ductility of these otherwise brittle compounds has made MA as a promising technique for the synthesis of high performance intermetallic compounds either

*Author for correspondence

directly by MA (Atzmon 1988; Calka and Radlinski 1990; Ivanov *et al* 1990; Shingu 1992; Cardellini *et al* 1993, 1994; Itsukaichi *et al* 1993; Mukhopadhyay *et al* 1994; Murty *et al* 1996; Pabi and Murty 1996; Pabi *et al* 1996) or by thermal treatment of mechanically alloyed powders (Benn *et al* 1988; Radlinski and Calka 1991; Murty 1992). However, reports on the mechanism of alloying during ball milling are relatively very few (Atzmon 1988; Zbiral *et al* 1992). By *in situ* measurement of vial temperature during MA in a SPEX mill, Atzmon (1988) reported that NiAl forms in the equiatomic mixture of Ni and Al through an explosive exothermic reaction similar to the self-propagating high temperature synthesis reaction (Munir 1992). Zbiral *et al* (1992) suggested that alloying in general occurs by the diffusion of either one element or both the elements depending on the equilibrium solid solubility. In an A–B system with significant solubility of B in A and relatively insolubility of A in B, alloying occurs by diffusion of B into A. In cases where the mutual solid solubility is appreciable, alloying seems to take place by diffusion of both the elements into each other. It is, however, not clear under what conditions such a diffusion model is applicable to the formation of compounds by MA. The present paper reports a systematic study of the mechanism of mixing in two model systems, namely, Ni–Al and Cu–Zn, that have widely different heats of formation (ΔH_f). In Ni–Al system, the intermetallic compounds like NiAl, Ni_3Al or Al_3Ni have large ΔH_f of > 120 kJ/mol (Kubaschewski *et al* 1967a). Moreover, NiAl is known to remain ordered up to its melting point, while Ni_3Al seems to have a relatively low ordering energy (5 kJ/mol) and low disordering temperature (638 K) (Aoki *et al* 1994; Koch and Cho 1992). In contrast, the intermetallic phases in Cu–Zn system are electron compounds with low ΔH_f (~ 8 kJ/mol) (Kubaschewski *et al* 1967b).

2. Experimental

High purity Ni and Al (99·9%) powders were mixed in the proportions of $Al_{100-x}Ni_x$($x = 10$, 18, 21, 25, 40, 50, 65, 68, 70, 75 and 90) and were mechanically alloyed in a Fritsch Pulverisette-5 planetary mill. A prealloyed powder of composition Al-50 wt.% Ni($Al_{70}Ni_{30}$) containing Al_3Ni, Al_3Ni_2 and NiAl phases was also ball milled under identical conditions with and without the addition of Al or Ni to achieve compositions of $Al_{100-x}Ni_x$($x = 10$, 18, 21, 25, 30, 40, 50, 65, 68, 70, 75 and 90). The milling was carried out at 300 rpm in WC container in toluene using 10 mm diameter WC balls with ball to powder weight ratio of 10:1. Similarly, elemental blends of Cu (99·9%) and Zn (99·5%) of compositions $Cu_{100-x}Zn_x$ ($x = 15$, 30, 40, 50, 65 and 85) were also mechanically alloyed. The effect of milling speed (200 vs 300), type of balls (steel vs WC) and milling atmosphere (dry vs wet) on the phase formation during MA were studied for the Cu–Zn system. Dry milling was carried out in air, while wet milling was performed in toluene. The mechanically alloyed powders were characterized by a Philips PW 1840 X-ray diffractometer with CuK_α radiation at regular intervals of milling. The crystallite size was calculated from X-ray diffraction (XRD) peak broadening, after separation of the contributions of strain and instrumental broadening by standard procedure (Guinier 1963). The crystallite size was confirmed by transmission electron microscopy (TEM) using Philips CM12 electron microscope.

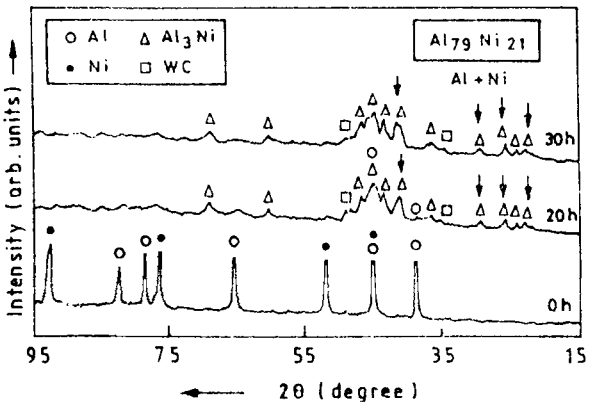

Figure 1. XRD patterns of $Al_{79}Ni_{21}$ blend as a function of milling time showing the evolution of Al_3Ni.

3. Results

3.1 *Synthesis of Ni aluminides by MA*

Nanocrystalline Al_3Ni, NiAl and Ni_3Al have been synthesized by MA in the present study. MA of elemental blend of $Al_{90}Ni_{10}$ composition has shown pure metal mixture of Al and Ni without any aluminide formation even after 30 h of milling. In contrast, $Al_{82}Ni_{18}$ and $Al_{79}Ni_{21}$ have shown the formation of Al_3Ni. Figure 1 shows the evolution of Al_3Ni in $Al_{79}Ni_{21}$ composition during MA. The residual Al present after 20 h of milling in this case completely disappeared on further milling up to 30 h. Some residual Al, however, persisted in the case of $Al_{82}Ni_{18}$ even after 30 h of MA. The superlattice reflections of Al_3Ni indicated by arrow-heads in figure 1 confirm that the Al_3Ni generated by MA remains ordered in the milled condition. The absence of shift in the XRD peaks of Al in these alloys suggests that ball milling is not effective in extending the solid solubility of Ni in Al.

Contrary to the expectations, MA of Al and Ni in stoichiometric ratio of Al_3Ni, i.e. $Al_{75}Ni_{25}$ blend has shown that Al_3Ni formed along with NiAl in the early stages (12 h) of milling disappears on further milling up to 20 h, leaving behind NiAl, as reported earlier (Murty *et al* 1996). Single phase NiAl was also found to be the end product of milling for $Al_{60}Ni_{40}$ and $Al_{50}Ni_{50}$ compositions. Figure 2 illustrates the evolution of NiAl in course of milling of $Al_{50}Ni_{50}$ elemental blend. Here the formation of NiAl can be noticed within 8 h of MA. Further milling, up to 16 h, resulted in the disappearance of XRD peak for Al, while the Ni peaks persisted up to 20 h. The NiAl produced in all the compositions was ordered, as manifested by the superlattice reflections (e.g. see arrow-head in figure 2). The nanocrystalline nature of the NiAl synthesized in the present study can be clearly seen from the TEM bright field image in figure 3. Average size of the particles was about 10 nm. The selected area electron diffraction pattern from these particles (inset of figure 3) confirms the absence of any amorphous phase.

MA of $Al_{35}Ni_{65}$ and $Al_{32}Ni_{68}$ has shown a two-phase mixture of ordered NiAl and disordered Ni_3Al. MA of Ni-rich compositions (70–90 at.% Ni) has yielded single phase disordered Ni_3Al. Formation of disordered Ni_3Al during MA is clearly evident from figure 4. No XRD peak shifts were observed for Al, while Ni peaks shifted

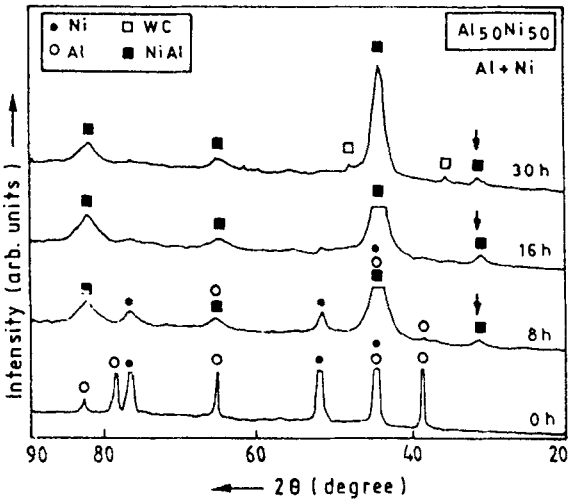

Figure 2. XRD patterns of $Ni_{50}Al_{50}$ blend at different milling times showing NiAl formation.

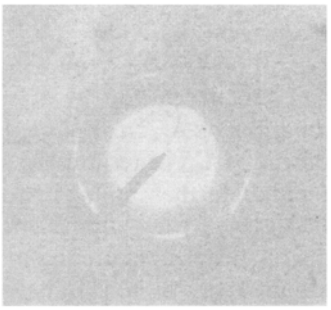

Figure 3. TEM bright field image of nanocrystalline NiAl. Inset shows the selected area diffraction pattern from NiAl.

continuously towards the Ni_3Al peak positions with increase in milling time. Within 20 h of milling, the peak positions matched closely with the fundamental lines of Ni_3Al and no peak shifts were observed with further milling. As the peak positions of the phase formed matched perfectly with the fundamental reflections of Ni_3Al in all the Ni-rich compositions studied (i.e. 70, 75 and 90 at.% Ni), the phase formed is referred to as disordered Ni_3Al rather than solid solution of Al in Ni, i.e. Ni(Al).

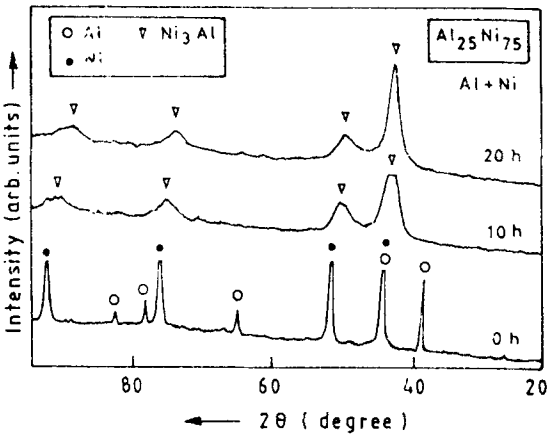

Figure 4. XRD patterns of $Al_{25}Ni_{75}$ at different milling intervals depicting the formation of disordered Ni_3Al.

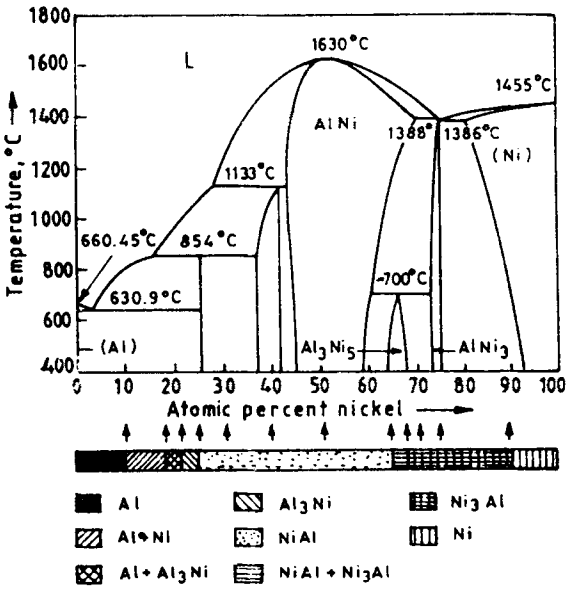

Figure 5. Ni–Al phase diagram showing the equilibrium phase fields of different aluminides. The bar below the phase diagram gives the large extension of phase fields of the aluminides obtained in Ni–Al system after 30 h of MA.

Figure 5 compares the phase field extensions obtained by MA for the aluminides with their equilibrium phase fields. Interestingly, while Al_3Ni is a line compound under equilibrium conditions, MA could result in its formation at compositions away from its stoichiometry. In the ball milled product, NiAl phase field manifests a large extension from 25–65 at.% Ni (equilibrium range is 45–58 at.% Ni). Similarly disordered Ni_3Al phase field has also been extended from 70–90 at.% Ni, as against the narrow equilibrium range of 74–76 at.% Ni for ordered Ni_3Al. The results of MA of mixture of alloy powder and Al or Ni with compositions $\geqslant 25$ at.% Ni are identical to those

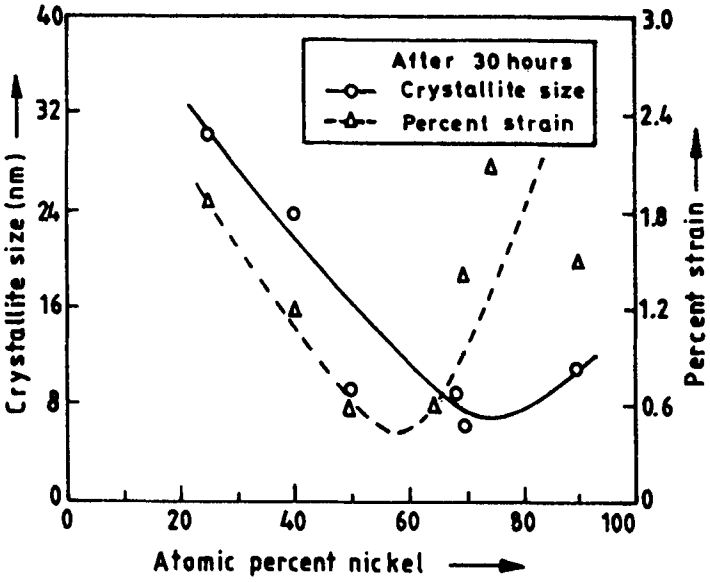

Figure 6. Variation of crystallite size and strain with composition in Ni–Al system after MA for 30 h.

obtained for pure metal mixture as shown in figure 5. For compositions < 25 at.% Ni, NiAl did not form by milling pure metal mixture, while in the case of mixture of alloy powder and Al, the NiAl present in the alloy powder could not be destabilized by prolonged (30 h) ball milling even in $Al_{90}Ni_{10}$ composition. However, it is interesting that, excepting the above fact, the other phases observed in the as milled condition were identical in both the cases.

The crystallite sizes and lattice strain after prolonged milling (~ 30 h) of different alloy compositions are shown in figure 6. It is interesting to note that crystallite size reaches a minimum (~ 6 nm) at the compositions where a two-phase mixture of NiAl and Ni_3Al coexists. The r.m.s strain appears to reach its minimum value near this range, possibly due to the ease of stress relaxation in smaller crystallite sizes. TEM study has confirmed that the crystallite size of Al_3Ni is larger than that of NiAl and the observed sizes are in good agreement with the values estimated from XRD data.

3.2 *Synthesis of electron compounds in Cu–Zn system by MA*

3.2a *Phase formation during MA*: Nanocrystalline ε, γ, β and α phases were synthesized by MA. Zn-rich phases were produced in the initial stages of MA process irrespective of the composition chosen. For example, in Cu-15 at.% Zn, the ε peaks were detected in the XRD pattern within 0·5 h of wet milling (figure 7). At this stage the crystallite size of Cu was quite coarse (> 200 nm). Upon prolonged milling, more stable Cu-rich phases formed, as is evident from figure 8. The sequence of phase formation at all the compositions studied in this system is shown in table 1.

A sharp rise in the Zn content in the Cu-rich α-solid solution was observed after α reached a crystallite size of about 15 nm (after ~ 4 h of milling), as shown in

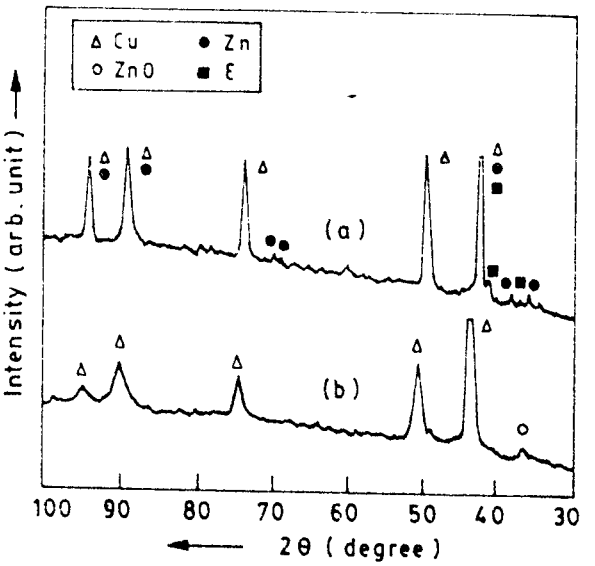

Figure 7. XRD patterns of Cu-15 at.% Zn after (a) 0·5 h and (b) 4 h of milling.

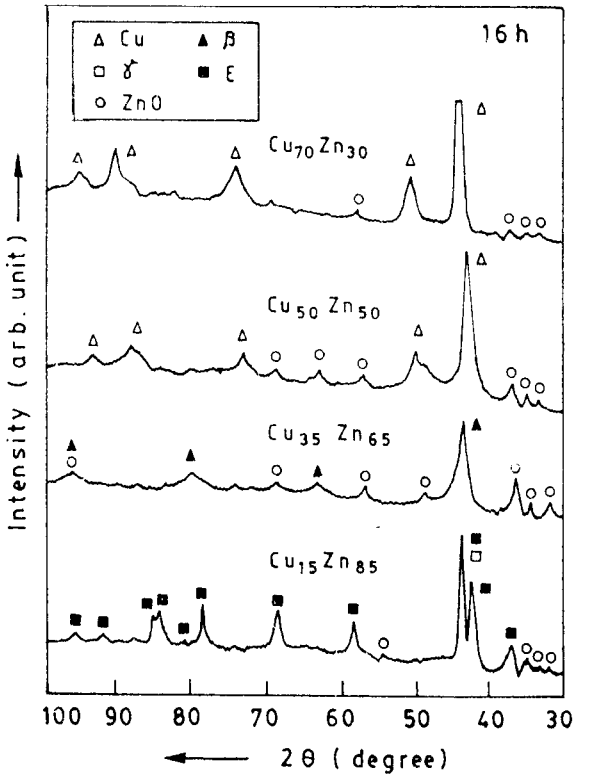

Figure 8. XRD patterns of different blends mechanically alloyed for 16 h.

Table 1. Transformation sequence during MA of different Cu–Zn blends.

Composition	Transformation sequence
$Cu_{85}Zn_{15}$	$\varepsilon \rightarrow \alpha + ZnO$
$Cu_{70}Zn_{30}$	$\varepsilon + \gamma \rightarrow \beta \rightarrow \alpha + ZnO$
$Cu_{60}Zn_{40}$	$\varepsilon + \gamma \rightarrow \beta + \alpha \rightarrow \alpha + ZnO$
$Cu_{50}Zn_{50}$	$\varepsilon + \gamma \rightarrow \varepsilon + \gamma + \beta \rightarrow \beta + M \rightarrow$ $\beta + \alpha + ZnO \rightarrow \alpha + ZnO$
$Cu_{35}Zn_{65}$	$\varepsilon + \gamma \rightarrow \gamma \rightarrow \gamma + \beta + ZnO \rightarrow \beta + ZnO$
$Cu_{15}Zn_{85}$	$\varepsilon \rightarrow \varepsilon + ZnO \rightarrow \varepsilon + \gamma + ZnO$

M, refers to martensite

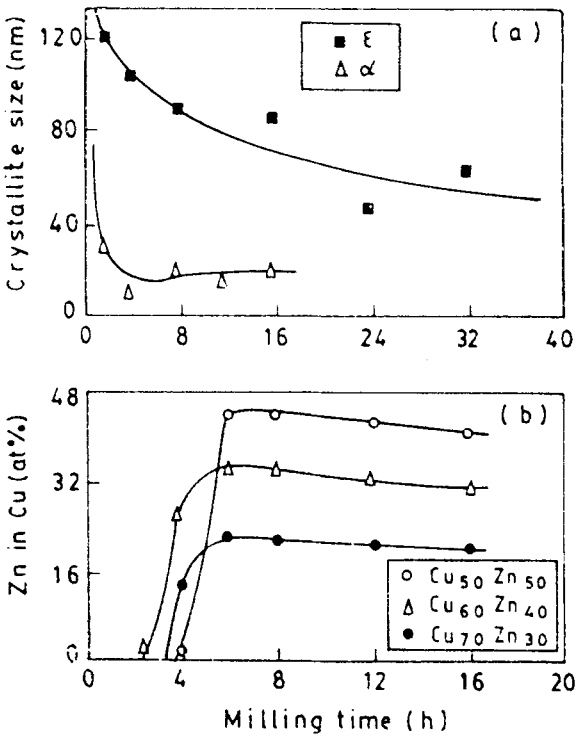

Figure 9. Change in (**a**) crystallite size and (**b**) Zn in Cu-solid solution, as a function of milling time.

figures 9 a and b. The milling time and the crystallite size at which this fast enrichment of Zn in α occurred, was found to be quite insensitive to the composition of the elemental blend up to 50 at.% of Zn. In these alloys the maximum amount of Zn in α in course of MA (figure 9b) increased with the increase in Zn content of elemental blend, as expected. A marginal extension of the α-phase field to $\sim$44 at.% Zn could be achieved in $Cu_{50}Zn_{50}$ blend. A gradual decrease of Zn in α was observed after milling beyond 8 h, which was associated with the formation of ZnO.

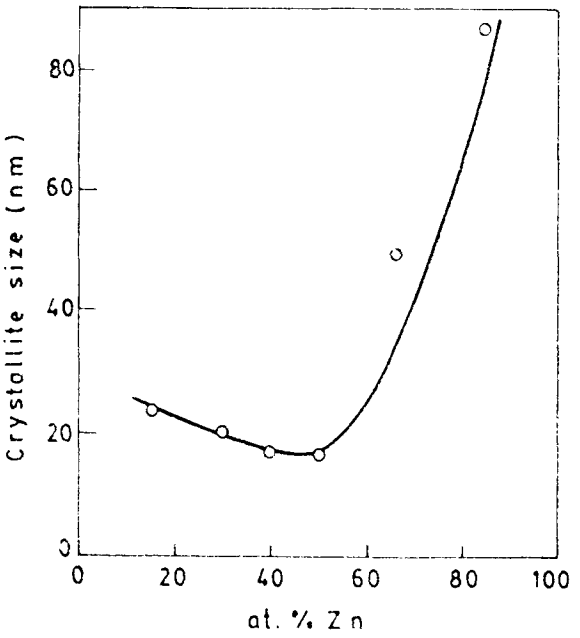

Figure 10. The crystallite size at different compositions after 16 h of milling.

At nominal compositions of 65 and 80 at.% Zn, β and ($\gamma + \varepsilon$) phases, respectively, were present after prolonged ($\sim$ 40 h) milling, while the equilibrium phase diagram predicts single phase γ and ε formation at these compositions. In fact, as the milling of these two blends continued beyond 8 h, the formation of Cu-rich phases was found to be associated with the oxidation of Zn-rich phases. A similar observation was reported in a recent work (Cardellini *et al* 1993) on elemental blends of Cu-80 and 85 at.% Zn. However, for nominal compositions of 50 at.% Zn or less, the Cu-rich phases were found to form by destabilization of Zn-rich phases. The ZnO formation in these alloys became significant only at a much later stage.

The crystallite size of Zn-rich ε phase decreased at a very slow rate with increase in the milling time when compared to α phase (figure 9a). For instance, after 40 h of milling, the crystallite size of ε phase was about 40 nm, while the α phase reached a crystallite size of $\sim$ 15 nm within 4 h of milling. This difference could be attributed to the difference in the melting points of the α and ε phases (Koch 1993), since the tendency for cold welding in the case of low melting phases is expected to be more. Among the different compositions studied, the crystallite size was found to reach a minimum ($\sim$ 18 nm) in the α-phase at the phase boundary of α and β (figure 10). A similar result was also observed in the Ni–Al system at the phase boundary of NiAl and Ni_3Al. It is also interesting to note that no such minimum is observed at the γ and ε phase boundary. These results probably suggest that the nanocrystalline mixtures of only the high melting phases mutually hinder the coalescence of crystallites.

Nanocrystalline nature of the alloys obtained by MA was confirmed by TEM studies. The crystallite size of α phase observed by TEM (figure 11) in $Cu_{50}Zn_{50}$ blend seems to be in good agreement with the average size of $\sim$ 18 nm as measured by XRD. The selected area electron diffraction pattern (inset of figure 11) corresponds to the α phase, and shows no evidence of amorphization.

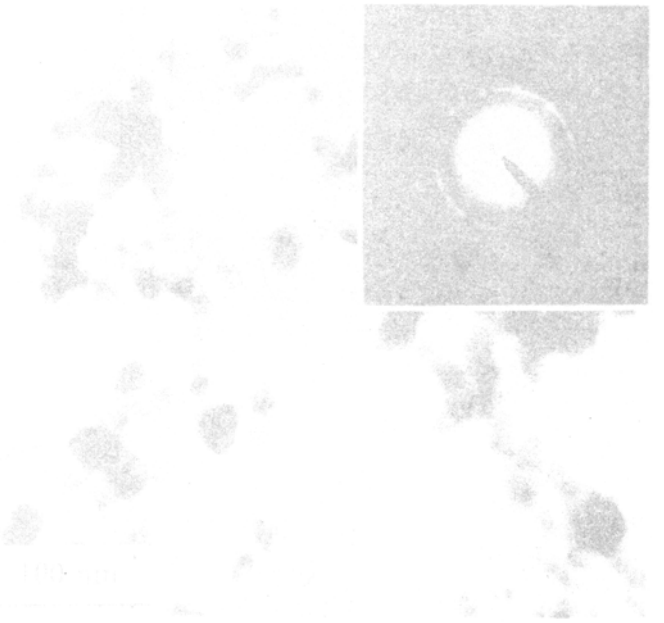

Figure 11. TEM bright field image of α in $Cu_{50}Zn_{50}$ milled for 16 h. Inset is the selected area diffraction pattern of the phase.

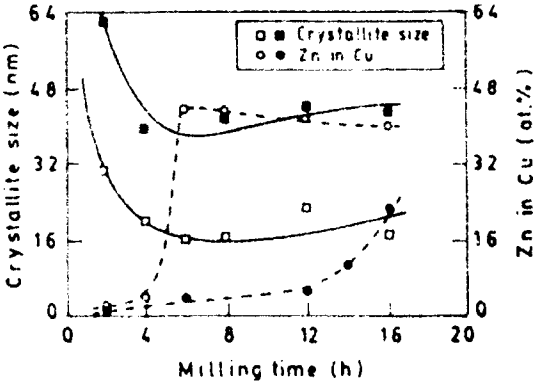

Figure 12. Time modulation of crystallite size (———) and Zn in Cu-solid solution (– – –) during dry (filled symbols) and wet (open symbols) milling of $Cu_{50}Zn_{50}$ blend.

3.2b *Effect of milling parameters*: A significant role of milling atmosphere on phase formation was evident from the dry and wet milling studies. While rapid alloying was observed on wet milling of $Cu_{70}Zn_{30}$, dry milling resulted in only oxide formation and no significant alloying could be detected even after 16 h of milling. In $Cu_{50}Zn_{50}$, formation of alloy phases was observed both in dry and wet milling conditions. However, during wet milling, a much more rapid crystallite size reduction and alloying (figure 12) were achieved as compared to dry milling of this composition. Sluggish rate of alloying in the dry milling operation is also associated with the early formation of

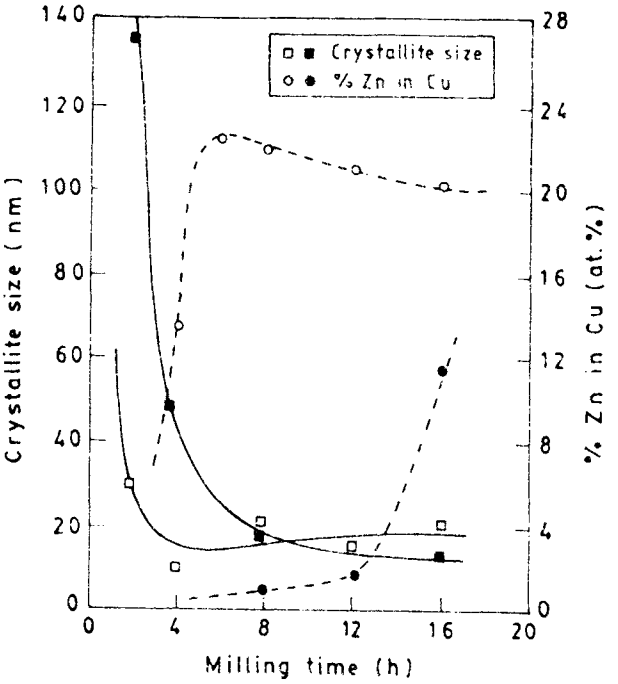

Figure 13. Crystallite refinement (——) and Zn content in α (- - -), as a function of time in $Cu_{70}Zn_{30}$ ball milled at 200 rpm (filled symbols) and 300 rpm (open symbols).

ZnO, as evidenced by the XRD results. Possibly the oxide layer acts as a barrier and retards or prevents the alloying process.

A comparative study of wet milling of $Cu_{70}Zn_{30}$ blend in steel grinding media, performed at different milling speeds of 200 and 300 rpm showed a faster drop in crystallite size in the initial stage of milling in the later case (figure 13). However, the final crystallite size of α after 16 h of milling was marginally lower at 200 rpm. This indicates that there is an optimum energy for grinding at which the fracture and cold welding processes strike a balance to yield the finest crystallite size in a system.

The contribution of higher energy imparted with WC medium is similar to that of higher milling speed, excepting the larger quantity of powder being employed in the former case for the same B/P ratio. Wet milling of $Cu_{70}Zn_{30}$ blend at B/P wt. ratio of 10:1 and milling speed of 300 rpm in WC media showed the formation of metastable strain induced martensite within 1 h of milling. Similar observation has been reported earlier (McDermott and Koch 1986) in the equiatomic blend. However, no such transformation could be detected in steel media. The higher specific gravity of WC as compared to steel imparts higher energy to the powder particles and probably introduces larger strain in the system sufficient to trigger the martensite formation. This martensite disappears during further milling possibly due to its compositional change. A much pronounced particle coarsening was observed in WC media after an initial drop in crystallite size (figure 14). This indicates more cold welding at higher milling energy. In $Cu_{70}Zn_{30}$ blend a marginal increase in the maximum Zn content in α to ~ 23·3 at.% (from 22 at.% in steel vial) was also achieved in WC medium (figure 8) apparently due to higher energy transfer in this medium.

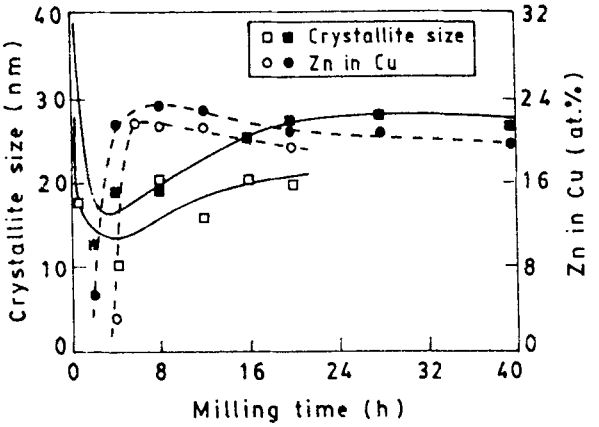

Figure 14. Change in crystallite size (———) and Zn content in Cu (– – –) in $Cu_{70}Zn_{30}$ blend milled in steel (open symbols) and WC (filled symbols) medium at different milling time.

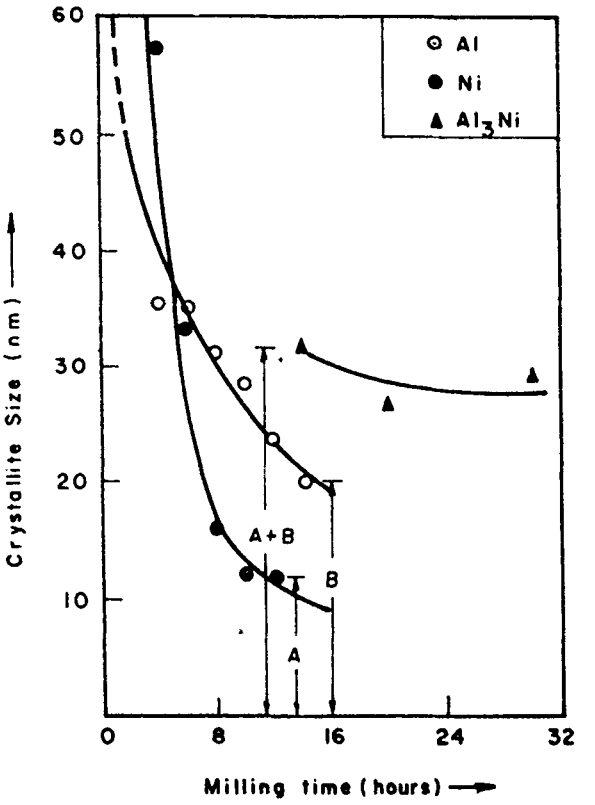

Figure 15. Variation of crystallite size of constituent metals with milling time during the formation of Al_3Ni in $Al_{79}Ni_{21}$ blend.

3.3 *Mixing phenomenon*

3.3a *Ni–Al system*: Observation of XRD patterns of different compositions in this system has shown that ordered Al_3Ni and NiAl form all of a sudden, while disordered

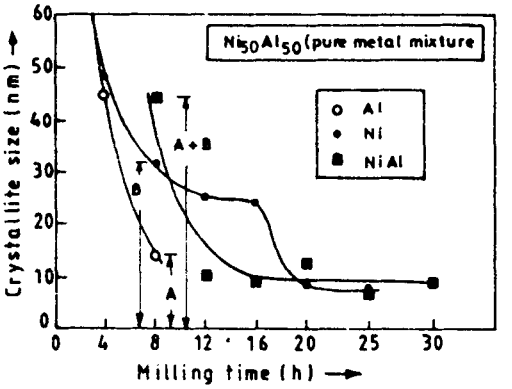

Figure 16. Variation of crystallite size of constituent metals with milling time during the formation of NiAl in $Al_{50}Ni_{50}$ blend.

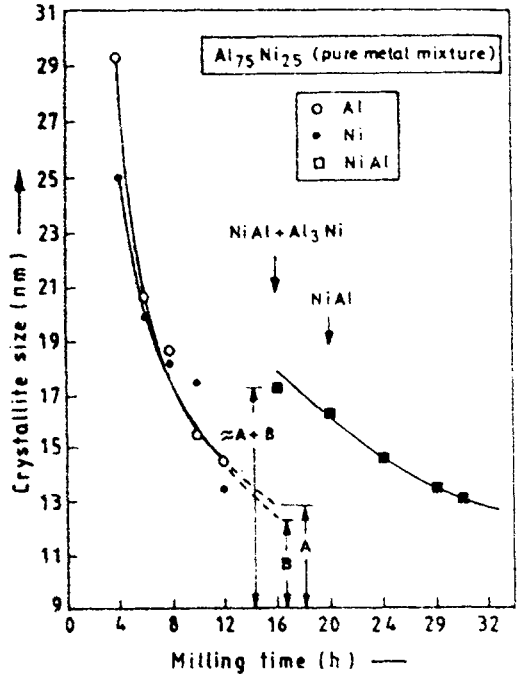

Figure 17. Variation of crystallite size of constituent metals with milling time during the formation of NiAl in $Al_{75}Ni_{25}$ blend.

Ni_3Al forms by continuous shifts in Ni peaks. Study of the crystallite sizes has evidenced the NiAl or Al_3Ni formation is triggered only when Al and Ni reach critical nanocrystalline sizes. In both the cases it was observed that the crystallite sizes of Al_3Ni and NiAl at the time of their formation, were equal to the sum of the crystallite sizes of their constituents (Al and Ni) as shown in figures 15 and 16, respectively. The critical crystallite sizes of Ni and Al required for the onset of NiAl formation in $Al_{50}Ni_{50}$ composition are found to be larger than that in $Al_{75}Ni_{25}$ (cf. figures 16 and 17).

3.3b *Cu–Zn system*: It is apparent from the present study on Cu–Zn system that irrespective of the blend composition, the Zn-rich ε and γ phases are first to form in the early stages of MA. Rapid diffusion of Zn into Cu and formation of α phase was observed only after Cu crystallites reached almost 15 nm size. Further, it appears that for compositions < 50 at.% Zn, the Cu-rich phases have formed by direct destabilization of Zn-rich phases due to diffusion of Cu, while in blends containing > 50 at.% Zn, the Cu rich phases seemed to form due to the loss of Zn from Zn-rich phases by oxidation. The pattern of XRD peak shift and crystallite size measurements reveal that the phases in Cu–Zn system form by diffusion of Cu and Zn in each other in course of milling in a manner similar to the mechanism of formation of disordered Ni_3Al. The only difference in these two cases is that in Cu–Zn system, diffusion of both Cu and Zn in each other was responsible for the formation of different phases, while the formation of disordered Ni_3Al was caused predominantly by the diffusion of Al into Ni.

4. Discussion

4.1 *Phase formation during MA*

The stability of Al_3Ni in blend compositions of $Al_{82}Ni_{18}$ and $Al_{79}Ni_{21}$, which deviate away from its stoichiometric composition ($Al_{75}Ni_{25}$), suggests that there could be some loss of Al due to oxidation in course of MA, thus shifting the alloy composition towards the stoichiometry of Al_3Ni. For similar reason Al_3Ni may become unstable during MA of $Al_{75}Ni_{25}$ blend. The chemical analysis of the mechanically alloyed samples reported in table 2 has confirmed this conjecture. A similar effect of oxidation has been reported earlier for Al–Fe system (Mukhopadhyay *et al* 1994), where Al_5Fe_2 (28 at.% Fe) forms by MA of an elemental blend of $Al_{75}Fe_{25}$ instead of the expected Al_3Fe. However, the stability of ordered Al_3Ni in nanocrystalline powders containing 22 to 24 at.% Ni is quite interesting in view of the fact that Al_3Ni is a line compound under equilibrium condition. This suggests that ordered Al_3Ni can accommodate some structural defects in Ni-sublattice induced by milling. However, milled Al_3Ni seems to be less tolerant to deficiencies in Al-sublattice, since it becomes unstable in ball milled alloys containing > 25 at.% Ni.

In contrast to Al_3Ni, the stability of ordered NiAl seems to be quite insensitive to both the compositional variations in binary system and the structural defects induced by MA. Similar results have also been reported by other investigators (Itsukaichi *et al* 1993; Cardellini *et al* 1994). Under ball milled condition nanocrystalline NiAl phase field could be extended more towards Al-rich side (up to 25 at.% Ni compared to equilibrium 45 at.% Ni) than towards Ni-rich side (i.e. up to 65 at.% Ni compared to 58

Table 2. Results of chemical analysis of milled powders of Ni–Al system.

Initial composition of elemental blend (at.% Ni)	Composition of powder milled for 30 h (at.% Ni)	Phases observed in XRD of milled product
18	22	Al + Al_3Ni
21	24	Al_3Ni
25	27	NiAl

at.% Ni in equilibrium diagram). This is in agreement with earlier studies on conventional NiAl structure, which show its more tolerance to vacancies in Ni-sublattice than Al-sublattice (Noebe *et al* 1993).

It may also be noted that the critical temperature of ordering T_c for NiAl varies in proximity of its melting point over a wide range of composition, and it declines only in the vicinity of NiAl–Ni_3Al phase boundary (Noebe *et al* 1993). Unlike the case of Al_3Ni or NiAl, the order parameter of Ni_3Al seems to be very sensitive to the structural defects induced by high energy ball milling, and Ni_3Al was disordered even at its stoichiometric composition. It is interesting to note that even after large number of investigations in this area (Atzmon 1988; Cardellini *et al* 1993; Itsukaichi *et al* 1993), there exists no report of direct synthesis of ordered Ni_3Al by MA. The low ordering energy (5 kJ/mol), low ordering temperature (638 K) (Koch and Cho 1992) and the close packed nature of the crystal structure seem to be the reasons for the easy destabilization of the order in Ni_3Al during milling. The extension of Ni_3Al in its disordered condition during MA (70–90 at.% Ni) in comparison to the equilibrium phase field of ordered Ni_3Al (74–76 at.%Ni) also could be related to the above reasons. Finally, the fact that the phases and phase fields obtained in Ni–Al system by MA are more or less identical for both types of starting blends, namely, pure metal mixtures and mixtures of alloy powder with Al or Ni, indicates that phases during MA arise out of thermodynamic reasons.

4.2 *Mechanism of alloying*

Present study on Ni–Al system shows that ordered NiAl and Al_3Ni form suddenly after individual constituents reach some critical nanocrystalline size. The sudden exothermic reaction in the vial to yield NiAl in $Ni_{50}Al_{50}$ mixture reported by Atzmon (1988) is a characteristic of reactive mixing. However, in a typical reactive mixing the zone of reaction usually spreads in an unrestrained fashion. In the present case, however, it is found that crystallite size of the ordered products is the sum of the individual crystallite sizes of Ni and Al, irrespective of the composition chosen. Hence, to distinguish this process from gradual diffusive or conventional reactive mixing, NiAl and Al_3Ni formation mechanism may be termed as 'discontinuous additive intermixing', as indicated in table 3. It is also conceivable that large scale and rapid intermixing of two constituents to yield an ordered product may involve a moving boundary process, once the product phase is nucleated.

In case of formation of an ordered reaction product like NiAl or Al_3Ni, the contribution of entropy change to the driving force may not be significant. Therefore, in these cases the larger the ΔH_f, the higher would be the driving force for the reaction. It

Table 3. Characteristic features of MA of Cu–Zn and Ni–Al systems.

System	Phase	ΔH_f(kJ/mol)	Product	Mode of mixing
Cu–Zn	ε	7	disordered	continuous diffusive
	α	8	disordered	continuous diffusive
Ni–Al	Al_3Ni	150	ordered	discontinuous additive
	NiAl	118	ordered	discontinuous additive
	Ni_3Al	153	disordered	continuous diffusive

is expected that the critical crystallite size at which such discontinuous mixing triggers, should diminish with the increase in driving force. This explains why critical crystallite sizes of Al and Ni for the formation of NiAl are higher in $Al_{50}Ni_{50}$, than in $Al_{75}Ni_{25}$. It is known that the ΔH_f of NiAl is maximum at its stoichiometric composition and decreases on either side (Noebe *et al* 1993).

In Ni_3Al, the ΔH_f is large (150 kJ/mol) and comparable to that for NiAl or Al_3Ni (Kubaschewski *et al* 1967a) (cf. table 3). However, Ni_3Al is unable to retain its ordered structure in ball milled condition possibly due to its low ordering energy (5 kJ/mol) (Aoki *et al* 1994). Since both Ni and disordered Ni_3Al are fcc, under ball milling condition, Ni_3Al loses its order and distinction with the solid solution of Al in Ni. This can explain why alloying in Ni–Al blends containing $\geqslant 70$ at.% Ni takes place by gradual enrichment of Ni with Al in a manner suggested by Zbiral *et al* (1992). It may be mentioned that the equilibrium solubility of Ni in Al is smaller when compared to Al in Ni. Hence, Al is expected to be the major diffusing species in a couple of Ni–Al. The absence of XRD peak shift for Al and the large peak shifts of Ni observed in course of MA support this mechanism. Table 3 summarizes the alloying characteristics of Ni-aluminides. It is apparent that disordered phase forms by continuous diffusive mixing during MA, even if ΔH_f is large.

In Cu–Zn system, the alloying was again observed to be by continuous diffusive mixing. This is expected, as ΔH_f of the phases in this system is quite low (8 kJ/mol) (Kubaschewski *et al* 1967b). However, it is interesting to note that alloying is initiated by the diffusion of Cu into Zn, while the reverse is expected from the solubility point of view. This is not difficult to understand, if one looks into the diffusivities of Cu and Zn in each other. It is clear from the simulation studies (Schwarz and Koch 1986) and the results of ball milling of Fe–C martensite (Davis *et al* 1988), that the local rise in temperature at the point of impact on a particle in a mill is not appreciable. Assuming a temperature of about 200°C, the diffusivities of Cu in Zn and Zn in Cu extrapolated from high temperature data are $3{\cdot}0 \times 10^{-18}$ and $8{\cdot}2 \times 10^{-27}$ m^2/s, respectively (Weast 1979). Since the diffusivity of Cu in Zn is about eight orders of magnitude higher than Zn in Cu, alloying is expected to initiate by the diffusion of Cu in Zn and the formation of Zn-rich phases such as ε and γ. Diffusion of Zn into Cu, and formation of α phase gains momentum only after the crystallite size of Cu is brought down to a few nanometers, so that the diffusion distances become small enough. Thus, it is observed from table 3, that the mode of mixing is continuous diffusive, if either the ΔH_f or the order energy is very low for any given compound. However, the major diffusing species in either case is decided by mutual solubilities and individual intrinsic diffusivities of the constituents.

5. Conclusions

(I) Nanocrystalline ordered Al_3Ni, NiAl and disordered Ni_3Al have been directly synthesized by MA. The phase fields of the above phases have been extended from 22–25, 25–65 and 70–90 at.% Ni, respectively. For a given composition, the metastable equilibrium achieved by ball milling seem to be insensitive to the structure of the starting blends.

(II) Stability of ordered Al_3Ni and, in particular, NiAl seem to be insensitive to the structural defects induced by milling, while ordered Ni_3Al was not stable under present milling conditions.

(III) Nanocrystalline solid solution (α) and electron compounds such as β, γ and ε could be generated in Cu–Zn system by MA.

(IV) The crystallite sizes are found to be dependent on the melting point and reached a minimum in the two-phase field of high melting, brittle compounds.

(V) The direct synthesis of ordered Al_3Ni or NiAl involving a large ΔH_f seems to take place through a discontinuous additive mixing mechanism. In contrast, when the ordering energy or heat of formation is low, the alloying apparently occurs through a continuous diffusive mechanism.

Acknowledgements

The work was sponsored by the Department of Science and Technology, Govt. of India (Grant No. III. 4(23)/92-ET). BSM is thankful for the financial assistance provided by ISIRD, IIT, Kharagpur. The technical help of Mr J Joardar, K H S Singh and P De is thankfully acknowledged.

References

Aoki K, Wang X M, Mcmezawa A and Masumoto T 1994 *Mater. Sci. Engg.* **A179/180** 390

Atzmon M 1988 *Phys. Rev. Lett.* **64** 487

Benjamin J S 1970 *Metall. Trans.* **1** 2943

Benn R C, Mirchandani P K and Watwe A S 1988 *Modern developments in powder metallurgy* (Princeton: MPIF) p. 479

Calka A and Radlinski A P 1990 *J. Less Common Metals* **161** L23

Cardellini F, Contini V, Mazzone G and Vittori M 1993 *Scr. Metall. Mater.* **28** 1035

Cardellini F, Mazzone G, Montone A and Antisare M V 1994 *Acta Metall. Mater.* **42** 2445

Das A and Pabi S K 1996 *Metals, Materials and Processes* (in press)

Davis R M, McDermott B T and Koch C C 1988 *Metall. Trans.* **A19** 2867

Gleiter H 1992 *Nanostructured Mater.* **1** 1

Guinier A 1963 *X-ray diffraction* (San Francisco: Freeman) p. 124

Itsukaichi T, Umemoto M and Moreno J G C 1993 *Scr. Metall. Mater.* **29** 583

Ivanov E, Grigorieva T, Gdubkova G, Boldyrev V, Fasman A B, Mikhailenko S D and Kalinina O T 1990 *Mater. Lett.* **7** 51

Koch C C 1991 *Processing of metals and alloys* (ed) R W Cahn (New York: VCH Publications) p. 193

Koch C C 1993 *Nanostructured Mater.* **2** 109

Koch C C and Cho Y S 1992 *Nanostructured Mater.* **1** 207

Kubaschewski O, Evans E L and Alcock C B 1967a *Metallurgical thermochemistry* (Oxford: Pergamon Press) p. 342

Kubaschewski O, Evans E L and Alcock C B 1967b *Metallurgical thermochemistry* (Oxford: Pergamon Press) p. 438

McDermott B T and Koch C C 1986 *Scr. Metall.* **20** 669

Miracle D B 1993 *Acta Metall. Mater.* **41** 649

Mukhopadhyay D K, Suryanarayana C and Froes F H 1994 *Scr. Metall. Mater.* **31** 333

Munir Z A 1992 *Metall. Trans.* **A23** 7

Murty B S 1992 *Study of amorphous phase formation by mechanical alloying in Ti based systems*, Ph. D Thesis, Indian Institute of Science, Bangalore

Murty B S 1993 *Bull. Mater. Sci.* **16** 1

Murty B S, Singh H S and Pabi S K 1996 *Bull. Mater. Sci.* **19** 565

Neiman G W, Weertman J R and Siegel R W 1991 *Clusters and cluster-assembled materials* (eds) R S Averback, J Bernholc and D L Nelson (Pittsburgh: MRS) p. 493

Noebe R D, Bowman R R and Nathal M V 1993 *Int. Mater. Rev.* **38** 193

Pabi S K and Murty B S 1996 *Mater. Sci. Engg.* **A214** 146

Pabi S K, Joardar J and Murty B S 1996 *J. Mater. Sci.* **31** 3207
Radlinski A P and Calka A 1991 *Mater. Sci. Engg.* **A134** 1376
Schwarz R B and Koch C C 1986 *Appl. Phys. Lett.* **49** 146
Shingu P H 1992 *Mechanical Alloying, Mater. Sci. Forum* **88–90**
Weast R C 1979 *CRC Handbook of Chemistry and Physics* (Ohio: CRC Press Inc.) **58** p. F-62
Zbiral J, Jangg G and Korb G 1992 *Mater. Sci. Forum* **88–90** 19